

# Interactions between Cardiac Glycosides and Sodium/Potassium-ATPase: Three-Dimensional Structure–Activity Relationship Models for Ligand Binding to the E<sub>2</sub>-P<sub>i</sub> Form of the Enzyme versus Activity Inhibition<sup>†</sup>

Stefan Paula,<sup>‡</sup> Michael R. Tabet, and William James Ball, Jr.\*

Department of Pharmacology and Cell Biophysics, College of Medicine, University of Cincinnati, Cincinnati, Ohio 45267

Received June 24, 2004; Revised Manuscript Received October 27, 2004

**ABSTRACT:** Sodium/potassium-ATPase (Na/K-ATPase) is a transmembrane enzyme that utilizes energy gained from ATP hydrolysis to transport sodium and potassium ions across cell membranes in opposite directions against their chemical and electrical gradients. Its transport activity is effectively inhibited by cardiac glycosides, which bind to the extracellular side of the enzyme and are of significant therapeutic value in the treatment of congestive heart failure. To determine the extent to which high-affinity binding of cardiac glycosides correlates with their potency in inhibiting pump activity, we determined experimentally both the binding affinities and inhibitory potencies of a series of 37 cardiac glycosides using radioligand binding and ATPase activity assays. The observed variations in key structural elements of these compounds correlating with binding and inhibition were analyzed by comparative molecular similarity index analysis (CoMSIA), which allowed a molecular level characterization and comparison of drug–Na/K-ATPase interactions that are important for ligand binding and activity inhibition. In agreement with our earlier comparative molecular field analysis studies [Farr, C. D., *et al.* (2002) *Biochemistry* 41, 1137–1148], the CoMSIA models predicted favorable inhibitor interactions primarily at the  $\alpha$ -sugar and lactone ring moieties of the cardiac glycosides. Unfavorable interactions were located about the  $\gamma$ -sugar group and at several positions about the steroid ring system. Whereas for most compounds a correlation between binding affinity and inhibitory potency was found, some notable exceptions were identified. Substitution of the five-membered lactone of cardenolides with the six-membered lactone of bufadienolides caused binding affinity to decline but inhibitory potency to increase. Furthermore, while the removal of ouabain's rhamnose moiety had little effect on inhibitory potency, it caused a dramatic decline in ligand binding affinity.

Cardiac glycosides in the form of digoxin and digitoxin (digitalis) have been an important component of the clinical treatment of congestive heart failure (CHF)<sup>1</sup> and supraventricular arrhythmias for many years (1–6). They exert their predominant therapeutic action through inhibition of the ion transport activity of the enzyme sodium/potassium-ATPase (Na/K-ATPase) in myocardial cells. Na/K-ATPase is a transmembrane protein that uses the chemical energy stored in ATP to derive the energy needed to transport potassium ions into and sodium ions out of eukaryotic cells against their natural gradients (7–9). The generation and maintenance of these ion concentration gradients are essential for many physiological processes. In myocardial cells, the

inhibition of Na/K-ATPase indirectly results in an elevation of intracellular calcium levels, producing an increase in the contractile force of the heart and cardiac output (inotropic effect) and thereby alleviating the symptoms of CHF.

Cardiac glycosides bind to Na/K-ATPase at a regulatory site that is located on the extracellular side on the  $\alpha$ -subunit of the enzyme (10, 11). Since Na/K-ATPase has multiple binding and release sites interacting with the transported ions, the inhibition mechanism of digitalis is quite complex and not that of a typical competitive inhibitor that simply blocks substrate access to the active site. Furthermore, during its catalytic cycle, Na/K-ATPase has been shown to adopt a number of different conformations (E<sub>1</sub> and E<sub>2</sub> forms), each with considerable differences in affinities for cardiac glycosides (12). A plausible mechanism for Na/K-ATPase inhibition is by digitalis-mediated paralysis of the movement of extracellular domains of the  $\alpha$ -subunit, particularly, the H5–H6 loop (13), that are required to remain flexible for the free interconversion between enzyme intermediates during the catalytic cycle. This type of inhibition mechanism has been observed for thapsigargin-mediated inhibition of the calcium-ATPase (14, 15), an enzyme closely related to Na/K-ATPase. For a thorough elucidation of the Na/K-ATPase inhibition mechanism or the development of novel inhibitors, detailed knowledge of the structural components of the inhibitors responsible for binding and for inhibition

<sup>†</sup> Support for this work came from the American Heart Association (Ohio Valley Affiliate, Grant 0051443B).

\* To whom correspondence should be addressed: 231 Albert Sabin Way, University of Cincinnati, Cincinnati, OH 45267-0575. Telephone: (513) 558-2371. Fax: (513) 558-1169. E-mail: william.ball@uc.edu.

<sup>‡</sup> Present address: Department of Chemistry, Northern Kentucky University, Highland Heights, KY 41099.

<sup>1</sup> Abbreviations: CHF, congestive heart failure; CoMFA, comparative molecular field analysis; CoMSIA, comparative molecular similarity index analysis; Na/K-ATPase, sodium/potassium-ATPase; C, number of components; QSAR, quantitative structure–activity relationship; RBA, relative binding affinity; RIP, relative inhibitory potency; PLS, partial least squares; E<sub>2</sub>-P<sub>i</sub>, phosphorylated E<sub>2</sub> conformation of Na/K-ATPase.

would be very valuable information. However, because of the absence of a high-resolution crystal structure, controversy about the exact location of the digitalis binding site, and a lack of knowledge of the interactions that govern inhibitor binding in various conformations of Na/K-ATPase, the molecular details of the inhibition mechanism remain elusive.

Structurally, cardiac glycosides are composed of three major components, a steroid ring system, a five- or six-membered lactone moiety, and at least one carbohydrate residue. A substantial number of studies with natural and synthetic cardiac glycosides have generated a body of evidence characterizing the effects of structural modifications on the inhibitory activities of these compounds on various isoforms of Na/K-ATPase (16–20). Most of the inhibitors that were tested in those studies displayed the conserved four-membered steroid ring system of the digoxin skeleton with modifications at the carbohydrate and lactone moieties and at selected positions of the steroid ring system. For example, Schönfeld *et al.* (21) reported structural variations of the carbohydrate groups that gave rise to a moderately diminished inhibitory potency. More recently, Cerri *et al.* (17, 18) showed that replacement of the lactone moiety of digoxin with functional groups containing basic amino groups connected to an  $\alpha,\beta$ -unsaturated spacer impairs Na/K-ATPase inhibitory potency. Our recent comparative molecular field analysis (CoMFA) study described several hormonal steroids whose lack of sugar and lactone moieties resulted in a reduced level of enzyme inhibition (22). None of these studies, however, has compared systematically binding affinities with inhibitory potencies, and with the exception of our recent three-dimensional QSAR study (22), contemporary computational tools have not been employed in identifying the crucial ligand–receptor interactions.

Here, we present a three-dimensional quantitative structure–activity relationship (3D-QSAR) study of the interactions that are crucial for high-affinity cardiac glycoside binding to the phosphorylated  $E_2$  enzyme conformation ( $E_2$ -P<sub>i</sub>) and inhibition of Na/K-ATPase activity using comparative molecular similarity index analysis (CoMSIA) modeling (23, 24). The models were based on experimental data obtained for a selection of 37 cardiac glycosides whose relative binding affinities and inhibitory potencies were obtained by competition radioligand binding and ATPase activity assays, respectively. CoMSIA is a relatively new method that adds hydrophobic and hydrogen bond (H-bond) fields to the classic steric and electrostatic CoMFA fields, thereby providing a more detailed specification of the nature of the intermolecular interactions (25). The CoMSIA contour maps identified the type and location of interactions that govern ligand binding and enzyme inhibition, respectively. Although we observed an overall correlation between binding and inhibition, we also noticed some important exceptions. The information gained from CoMSIA modeling provides important information for a more complete understanding of the molecular details of digitalis binding and digitalis-mediated Na/K-ATPase inhibition and is potentially valuable for the future design of novel cardiac glycoside-based therapeutic agents.

## EXPERIMENTAL PROCEDURES

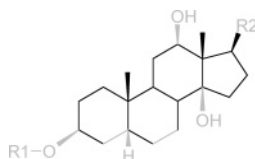
**Materials.** The cardiac glycosides digoxigenin bisdigitoxoside, digitoxigenin bisdigitoxoside, and digitoxigenin

monodigitoxoside were obtained from Roth (Karlsruhe, Germany).  $\alpha$ -Methyldigoxin,  $\alpha,\beta$ -diacetyldigoxin,  $\beta$ -acetyldigoxin, strophanthidin, lanatoside A, and evomonoside were from Boehringer (Ingelheim, Germany). Lanatoside B and uzarigenin were from Pfaltz & Bauer (Waterbury, CT). 16-Acetylgitoxin was from Indofine (Hillsborough, NJ). Digoxigenin monodigitoxoside was from Glaxo Wellcome (Research Triangle Park, NC). Anthrolyouabain was from Molecular Probes (Eugene, OR). Radiolabeled ouabain [<sup>3</sup>H(G)]ouabain; specific activity of 18 Ci/mmol} was purchased from Perkin-Elmer (Boston, MA). All other compounds, reagents, and enzymes for the ATPase activity assays were received from Sigma-Aldrich (St. Louis, MO).

**Na/K-ATPase Purification.** Na/K-ATPase was isolated from the outer medulla of lamb kidneys according to the method of Lane *et al.* (26). The protein concentration was determined by the method of Lowry (27) using bovine serum albumin as the protein standard. The ATPase activity of the purified enzyme was determined according to the assay described below (28, 29) and gave a specific activity of approximately 380  $\mu\text{mol mg}^{-1} \text{h}^{-1}$ . The purity of the enzyme preparation was verified by SDS–PAGE, which showed only two bands, one at 110 kDa and the other at 55 kDa, indicative of the  $\alpha$ - and  $\beta$ -subunits, respectively, after staining with Coomassie blue.

**Radioligand Assay of Cardiac Glycoside Binding by Na/K-ATPase.** The binding affinity of Na/K-ATPase for ouabain ( $K_d$ ) was determined by saturation radioligand binding assays using a previously described filtration method with some minor modifications (28, 29). A dilution series of [<sup>3</sup>H]ouabain was prepared by adding small aliquots of a 1  $\mu\text{M}$  stock solution of [<sup>3</sup>H]ouabain in water to 5 mL of a freshly prepared Na/K-ATPase solution (final concentration of 1 nM) in assay buffer [50 mM Tris-HCl, 5 mM MgCl<sub>2</sub>, 5 mM Tris-phosphate, and 0.1 mM EGTA (pH 7.4) (final concentrations)]. These conditions are known to induce the  $E_2$ -P<sub>i</sub> conformation of Na/K-ATPase, which is the conformation with the highest affinity for cardiac glycosides (as compared to buffers containing Mg<sup>2+</sup>/ATP or Mg<sup>2+</sup> only). After the mixture had been shaken for 120 min at room temperature, the binding equilibrium was reached and the individual samples were passed through glass fiber filters (type B, Schleicher and Shuell, No. 32) using a Brandel cell harvester with 96 sampling probes. Tubes and filters were rinsed three times with 8 mL aliquots of ice-cold assay buffer. The amount of radioactivity retained by the filters was determined by liquid scintillation counting (LS7500, Beckman). To account for nonspecific [<sup>3</sup>H]ouabain binding to the filters, control samples without Na/K-ATPase but otherwise identical were monitored. Each data point was the average of two independent measurements, and each experiment was repeated three times. Dissociation constants ( $K_d$ ) were determined by fitting the measured counts per minute as a function of total ouabain concentration to a binding isotherm.

The binding affinities of nonradioactive cardiac glycosides relative to [<sup>3</sup>H]ouabain were obtained by a competition assay. The experimental conditions were identical to those described above, except that nonradioactive competitors were present at eight different concentrations and the concentration of [<sup>3</sup>H]ouabain was kept constant at either 2 nM (using 2 nM Na/K-ATPase) or 0.2 nM (using 0.2 nM Na/K-ATPase), depending on the affinity of the respective competitor.

Scheme 1: Alignment Template<sup>a</sup>

<sup>a</sup> All compounds were superimposed on the black part of the digoxin cardenolide system.

Because of the low off-rate of cardiac glycosides, the incubation time was increased to a minimum of 16 h to allow for equilibration. The radioactive counts as a function of competitor concentration from experiments performed in duplicate were fit to a three-parameter logistic equation according to the method of Cheng and Prusoff (30). IC<sub>50</sub> values were the concentrations of the competitor required to displace half of the [<sup>3</sup>H]ouabain initially bound to the Na/K-ATPase.

**Na/K-ATPase Activity Inhibition Assay.** Inhibitory potencies of cardiac glycosides were determined by assaying the ATPase activity of the purified Na/K-ATPase (31) at 10 different inhibitor concentrations. In a plastic cuvette, the enzyme (20–40  $\mu$ L of a 0.1 mg/mL stock solution) and the inhibitor were incubated for at least 20 min at 37 °C in an assay mixture [100 mM NaCl, 45 mM histidine, 10 mM KCl, 10 mM MgCl<sub>2</sub>, 1 mM phosphoenolpyruvate, and 0.23 mM NADH (pH 7.3)] containing pyruvate kinase and lactate dehydrogenase (12 and 8.4 units/mL, respectively; final volume of 1.25 mL). After checking for potential background rates of NADH oxidation, the reaction was started by adding ATP (final concentration of 5 mM). Rates of the rate-limiting NADH oxidation were determined spectroscopically for 7 min with a UVIKON 930 spectrophotometer operating at a wavelength of 340 nm and converted into specific activities.

ATPase activities as a function of inhibitor concentration were fit to a three-parameter logistic equation (amplitude, offset, and IC<sub>50</sub>), and the relative inhibitory potency (RIP) of a compound was expressed as its IC<sub>50</sub> value divided by the IC<sub>50</sub> value of ouabain. The IC<sub>50</sub> was the concentration of inhibitor that caused inhibition of half of the ATPase activity observed in the absence of inhibitor. All experiments were performed in duplicate at least three times, and only compounds capable of inhibiting ATPase activity by more than 90% were used for further analysis.

**Molecular Modeling and Structural Alignment of Cardiac Glycosides.** Molecular modeling was performed with the SYBYL software package from Tripos (version 6.9). The molecular structure of digoxin was extracted from the crystal structure of its complex with murine monoclonal antibody fragment 26-10 [Protein Data Bank (PDB) entry 1IGJ (32)]. As described previously (22, 33), the extracted digoxin structure was then subjected to a systematic conformational search of all rotatable bonds (10° increments) and molecular mechanics energy minimization, using the MMFF94s force field, MMFF94s charges, a distance-dependent dielectric constant of 4, and a conjugate gradient optimizer with a convergence criterion of 0.01 kcal mol<sup>-1</sup> Å<sup>-1</sup>. Other cardiac glycosides were modeled by substituting the appropriate residues in the digoxin structure and repeating the force field minimization procedure.

The structures of all compounds were aligned by superimposition onto a template by means of a least-squares

procedure. Because of its presence in all compounds that were tested, the part of the steroid ring system shown in black in Scheme 1 below served as the alignment template. Further, while there can be rotation about the glycoside and the steroid–lactone bonds and some compounds may assume alternate steroid ring A conformations (34), we have assumed the same conformation for each bound ligand. This type of alignment and the assumed single conformation have been used successfully by us and others in previous 3D-QSAR studies of steroid-based drugs (22, 33, 35, 36).

**Comparative Molecular Similarity Index Analysis of Cardiac Glycoside Binding Affinity for and Inhibition of Na/K-ATPase.** CoMSIA modeling was performed with the QSAR module of SYBYL as described previously (23, 24, 36). Briefly, the five molecular fields (steric, electrostatic, lipophilic, H-bond donor, and H-bond acceptor) were calculated by computing molecular similarity indices between the cardiac glycosides and a probe atom placed on the intersection points of a 3D grid according to (23)

$$A_{F,k}^q(j) = -\sum_i w_{\text{probe},k} w_{ik} e^{-\alpha r_{iq}^2}$$

At grid point  $q$  (2 Å spacing interval),  $A$  represents the molecular similarity index of molecular field  $F$  calculated for all atoms (summation index  $i$ ) of compound  $j$  and a probe atom.  $r_{iq}$  is the distance between the probe atom at grid point  $q$  and atom  $i$  of the compound.  $w_k$  is a parameter describing the appropriate physicochemical property ( $k$ ) of compound  $j$  and the probe atom (radius of 1 Å, charge of +1, hydrophobicity index of +1, H-bond donating parameter of +1, and H-accepting parameter of +1) at each grid point. For the steric field,  $w_k$  is the third power of the atomic radius. For the electrostatic field,  $w_k$  represents the electrostatic charges. For the hydrophobic field,  $w_k$  is equal to the atom-based hydrophobicity parameter according to Viswanadhan (37). For H-donor and H-acceptor fields,  $w_k$  reflects a value assigned to suitably placed pseudoatoms (23). The attenuation factor  $\alpha$  in the exponent was set to its default value of 0.3 (23).

Correlations between the biological activities (binding affinity or inhibitory potency) and the molecular fields of the compounds were established by the partial least-squares (PLS) method implemented in SYBYL. PLS expresses the information contained in the large number of molecular field descriptors in the more compact form of a few principal components that are linear combinations of the original descriptors. Using SYBYL's SAMPLS feature (38), the optimum number of components was defined as the value that corresponded to a cross-validated correlation coefficient ( $r_{cv}^2$ ) that did not increase by more than 5% upon addition of a further component. The following non-cross-validated PLS analyses were carried out with this number of components. All PLS runs were executed with SYBYL's "CoMFA standard scaling" feature activated and with a column filter set to 2 kcal/mol for the purpose of noise reduction.

The predictive power of the developed CoMSIA models was determined by performing the PLS analysis with the exclusion of three different sets containing four test compounds each [see the Supporting Information (Table 3)]. These particular test compound sets were randomly selected,



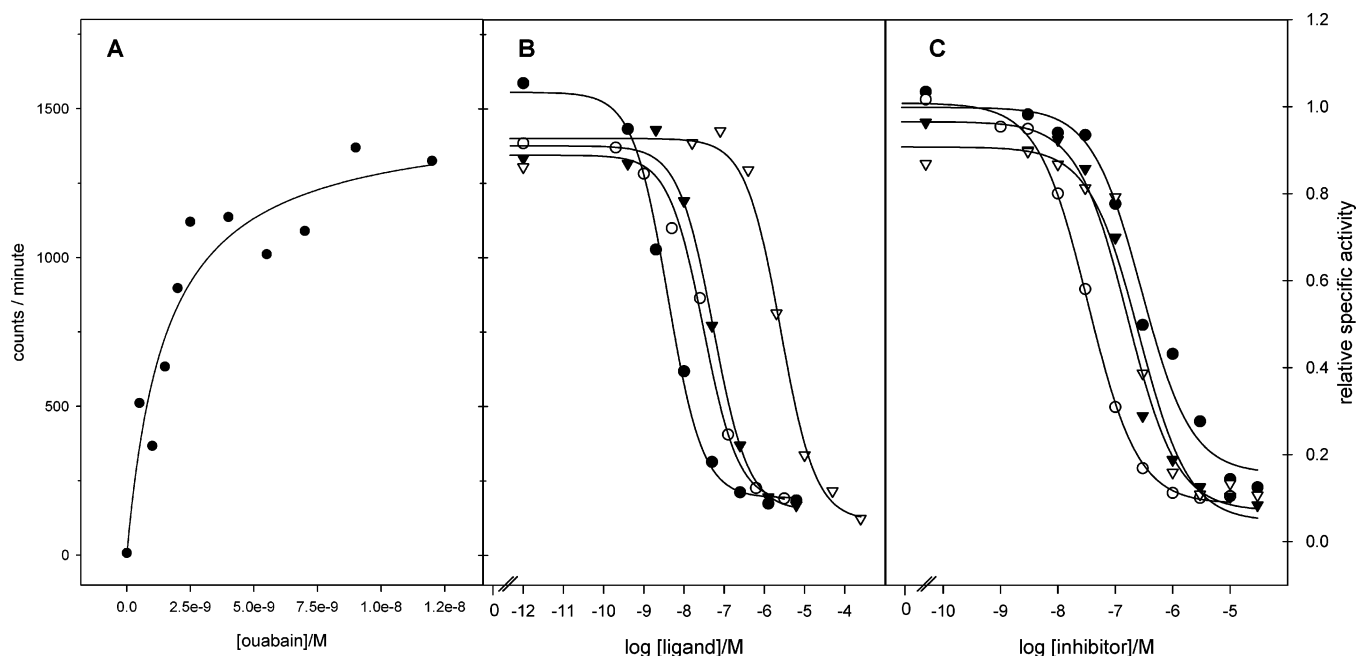


FIGURE 1: Representative radioligand binding and ATPase activity inhibition assays. (A) Determination of the  $K_d$  for binding of [ $^3\text{H}$ ]-ouabain to Na/K-ATPase. (B) Competition assay with nonradioactive cardiac glycosides and [ $^3\text{H}$ ]ouabain. (C) ATPase activity assay in the presence of inhibitors. Symbols [(●) ouabain, (○) bufalin, (▼) strophanthidin, and (△) ouabagenin] represent the average of two independent experimental trials.

except for ensuring a range in their activity values, and were different for the two assay data sets. The ability of the models to properly predict the RBA and RIP values of “unknown” molecules served as a measure of the external predictive ability of the model.

## RESULTS

**Relative Binding Affinities of Cardiac Glycosides for Na/K-ATPase.** As shown in Figure 1A, a saturation radioligand binding assay was used for the determination of the dissociation constant ( $K_d$ ) of [ $^3\text{H}$ ]ouabain and Na/K-ATPase. The  $K_d$  value of  $2.2 \pm 0.8$  nM ( $n = 3$ ) obtained for the purified lamb kidney enzyme was in agreement with previously reported results (1.4–2.0 nM) for conditions favoring the high-affinity  $\text{E}_2\text{-P}_i$  form of the enzyme, which is achieved by the presence of magnesium and phosphate ions (29, 39, 40). When carried out in the competition mode, the assay also permitted the determination of  $\text{IC}_{50}$  values of non-radioactive cardiac glycosides versus that of ouabain ( $\text{IC}_{50} = 5.4 \pm 2.0$  nM,  $n = 46$ ; Figure 1B) for the generation of 3D-QSAR models. Since relative rather than absolute affinity values are used for the model development, all  $\text{IC}_{50}$  values were converted to relative binding affinities (RBAs). The RBA was defined as the ratio of the  $\text{IC}_{50}$  value of a given compound divided by that of ouabain. Thus, a RBA value of  $>1$  indicates a binding affinity lower than that of ouabain and a RBA value of  $<1$  an affinity greater than that of ouabain.

For the selected set of 37 cardiac glycosides (structures in Table 1), the experimentally determined RBAs covered a range of more than 3 orders of magnitude with evomonoside (RBA = 0.13) and proscillaridin A (RBA = 0.45) as the highest-affinity binders and ouabagenin (RBA = 311) and chlormadinone acetate (RBA = 147) as the lowest-affinity binders (see Table 2). A wide spread in affinities is in general advantageous for the detection of structure–activity trends and the development of robust QSAR models. Whereas a

comprehensive description using 3D-QSAR methodology is presented in the Discussion, we briefly summarize here the most prominent effects of structural modifications on the binding affinities of ligands.

Within our data set, the most dramatic changes in RBA occur as a result of modifications of the lactone moiety. The saturation of the lactone ring, as exemplified in the compound pair ouabain/dihydroouabain and digoxin/dihydrodigoxin, causes an increase in RBA values of almost 2 orders of magnitude. As reported previously (22), this seemingly minor structural modification abolishes the planarity of the lactone ring system and may result in a repositioning of the compound in the binding pocket of Na/K-ATPase. Likewise, the substitution of the five-membered ring with a six-membered lactone ring in the bufadienolides bufalin and evomonoside reduces binding affinity as compared to their congeners digitoxigenin and proscillaridin A, although to a lesser extent (2–4-fold) than observed for the two previous compounds.

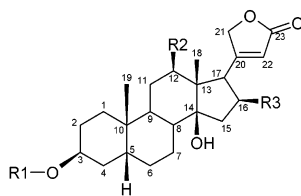
Another structurally important feature is the *cis*–*trans* stereochemistry of the bond between C-5 and C-10, connecting steroid rings A and B. As is evident from uzarigenin’s 25-fold lower binding affinity compared to digitoxigenin, a *cis* ring fusion is more favorable for high-affinity binding than the *trans* fusion, but not absolutely essential.

The significance of the  $\alpha$ -,  $\beta$ -, and  $\gamma$ -digitoxose residues can be assessed by inspection of RBAs in the digoxin- and digitoxin-based compound series that vary systematically in the number of carbohydrate monomers. Provided that at least one digitoxose is present, the RBA values increase moderately with an increasing number of carbohydrate moieties. On the other hand, the removal of all carbohydrates (genins) causes the affinity to decrease by approximately 1 order of magnitude.

Inspection of data for cardiac glycosides with identical cardenolide but different monosugar moieties permits the

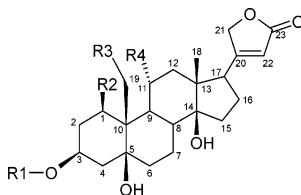
Table 1: Chemical Structures of Cardiotonic Steroids

## Digitoxigenin-Based Compounds



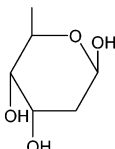
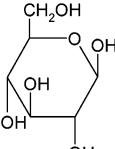
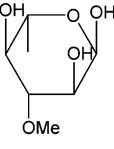
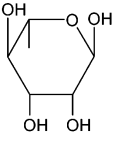
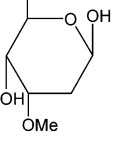
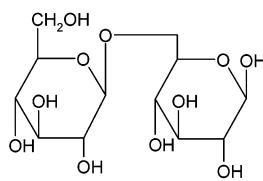
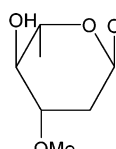
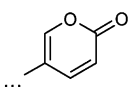
name	R1	R2	R3	other
digitoxin	trisdigitoxose	—H	—H	—
digitoxigenin bisdigitoxoside	bisdigitoxose	—H	—H	—
digitoxigenin monodigitoxoside	monodigitoxose	—H	—H	—
digitoxigenin	—H	—H	—H	—
digoxin	trisdigitoxose	—OH	—H	—
digoxigenin bisdigitoxoside	bisdigitoxose	—OH	—H	—
digoxigenin monodigitoxoside	monodigitoxose	—OH	—H	—
digoxigenin	—H	—OH	—H	—
$\alpha$ -methyl digoxin	trisdigitoxose	—OH	—H	$\alpha$ -methyl at C-3' of third digitoxose
$\alpha,\beta$ -diacetyldigoxin	digitoxose bisdigitoxose	—OH	—H	$\alpha,\beta$ -bisacetyl at C-3' of third digitoxose
$\beta$ -acetyldigoxin	trisdigitoxose	—OH	—H	$\alpha$ -acetyl at C-3' of third digitoxose
gitoxin	trisdigitoxose	—H	—OH	—
gitoxigenin	—H	—H	—OH	—
gitoxigenin 3,16-diacetate	CH <sub>3</sub> CO—	—H	—OCOCH <sub>3</sub>	—
16-acetyl gitoxin	trisdigitoxose	—H	—OCOCH <sub>3</sub>	—
lanatoside A	monoglucose trisdigitoxose	—H	—H	—OCOCH <sub>3</sub> at C-3' of third digitoxose
lanatoside B	monoglucose trisdigitoxose	—OH	—OH	—OCOCH <sub>3</sub> at C-3' of third digitoxose
lanatoside C	monoglucose trisdigitoxose	—OH	—H	—OCOCH <sub>3</sub> at C-3' of third digitoxose
dihydrodigoxin	trisdigitoxose	—OH	—H	C-20—C-22 saturated
evomonoside	rhamnose	—H	—H	—
neriifolin	thevetose	—H	—H	—
thevetin B	thevetose gentiobiose	—H	—H	—H
bufalin	—H	—H	—H	six-membered lactone
cinobufagin	—H	—H	—OCOCH <sub>3</sub>	six-membered lactone, C-14—C-15 epoxide, —OH at C-5
uzarigenin	—H	—H	—H	C-5—C-10 <i>trans</i>
oleandrin	oleandrose	—H	—OCOCH <sub>3</sub>	—H
oleandrigenin	—H	—H	—OCOCH <sub>3</sub>	—H
prosillaridin A	rhamnose	—H	—H	six-membered lactone, C-4—C-5 double bond
chlormadinone acetate	=O	—H	—H	C-4—C-5 and C-6—C-7 double bonds, $\alpha$ -OCOCH <sub>3</sub> , and $\beta$ -COCH <sub>3</sub> at C-17

## Ouabagenin-Based Compounds



name	R1	R2	R3	R4	other
ouabagenin	—H	—OH	—OH	—OH	—
ouabain	rhamnose	—OH	—OH	—OH	—
strophanthidin	—H	—H	=O	—H	—
strophanthidol	—H	—H	—OH	—H	—
cymaroside	cymarose	—H	=O	—H	—
helveticoside	digitoxose	—H	=O	—H	—
anthrolyouabain	9-anthracene carbonyl-3'-rhamnose	—OH	—OH	—OH	—
dihydroouabain	trisdigitoxose	—OH	—OH	—OH	C-20—C-22 saturated
peruvoside	thevetose	—H	=O	—H	—

Table 1: (Continued)

Other Residues					
					
digitoxose	glucose	thevetose	rhamnose	cymarose	
					
gentiobiose		oleandrose		six-membered lactone	

assessment of the importance of the specific type of sugar for binding to the enzyme. The RBA values of the digitoxin-based compounds evomonoside (rhamnose), digitoxigenin monodigitoxoside (digitoxose), and neriifolin (thevetose) differ by a factor of no more than 3, which is a rather small effect. Interestingly, the RBA of the gitoxin-based compound helveticoside (digitoxose) is almost 2 orders of magnitude larger than that of cymar in (cymarose), whose affinity is comparable to those of the digitoxin-based monosaccharides. The most interesting observation relates to the large decrease in binding affinity upon removal of the rhamnose moiety of ouabain (RBA for ouabagenin = 311), which agrees with an earlier report (39). This implies an important contribution of rhamnose to ouabain binding since it apparently compensates for an intrinsically unfavored binding of the hydroxyl group-rich “genin” moiety of ouabain. The specific ability of rhamnose to enhance binding is also observed upon its addition to digitoxigenin, yielding evomonoside, which produces a substantial 18-fold increase in affinity.

The introduction of hydroxyl groups in positions C-12 and C-16 at the steroid skeleton (digoxin and gitoxin derivatives, respectively) generally results in a slight reduction in binding affinity, which is observed consistently, but the effect is typically smaller than 1 order of magnitude. If an acetyl instead of a hydroxyl group is introduced at C-16, this effect is reversed; i.e., the affinity slightly increases.

Other modifications bear little significance for binding to Na/K-ATPase, such as modifications of the  $\gamma$ -sugar ( $\alpha$ -methyl digoxin, diacetyldigoxin,  $\beta$ -methyl digoxin, or acetyl-digitoxin), the attachment of an anthracene group to the rhamnose moiety of ouabain (anthrolyouabain), or the reduction of the aldehyde function at C-19 of strophanthidin to yield strophanthidol.

**Relative Inhibitory Potencies of Cardiac Glycosides.** Using an ATPase activity assay, we also determined the  $IC_{50}$  values for Na/K-ATPase activity inhibition (Figure 1C) for the same selection of cardiotonic steroids under the lower-affinity conditions. For the 3D-QSAR modeling, the  $IC_{50}$  values were converted to relative inhibitory potencies (RIPs) by dividing the  $IC_{50}$  of each compound by that of ouabain ( $209 \pm 104$  nM,  $n = 13$ ). The set of compounds tested is an expansion of that used in our earlier study (22), and a comparison of

RIP results of compounds present in both sets revealed good agreement. Interestingly, the RIP values covered a range of only  $\sim 2$  orders of magnitude, which is smaller than that seen for the binding affinity values. Evomonoside (RIP = 0.06) and proscillaridin A (RIP = 0.11) were the most potent inhibitors, whereas chormadinone acetate (RIP = 21) and dihydrodigoxin (RIP = 7.1) were the least potent compounds.

Inspection of the RIP/RBA ratio data of Table 2 reveals those compounds that have an inhibitory potency different from what would be expected on the basis of their binding affinity (using ouabain as the standard, RIP/RBA ratio = 1). Compounds with unexpectedly high inhibitory potencies are ouabagenin, uzarigenin, and bufalin (RIP/RBA ratio = 140, 42, and 36, respectively). Compounds that proved to be poor inhibitors were peruvoside,  $\beta$ -acetyldigoxin, and neriifolin, although the mismatch here was much smaller (RIP/RBA ratio = 0.31, 0.34, and 0.37, respectively). The identification of these outliers as well as the illustration of the good correlation between RIP and RBA for most test compounds is visualized in the plot of  $-\log$  RIP versus  $-\log$  RBA values in Figure 2.

Overall, most of the major trends regarding changes in RIP as a consequence of structural modification are also observed in the RBA data. Perhaps the most noticeable deviation occurs with an increase in the size of the lactone ring from five to six atoms (digitoxigenin/bufalin and evomonoside/proscillaridin A pairs), which improved inhibitory potency but decreased binding affinity. Another difference relates to the fact that compared to compounds with sugar moieties, the genins are about equally or slightly more (in the case of digoxin-based inhibitors) active inhibitors. Furthermore, the effects of lactone ring saturation and of *cis-trans* stereochemistry of the C-5–C-10 bond are less drastic for activity inhibition than for binding. Whereas a small increase in RIP upon addition of a hydroxyl group at C-12 is equivalent to the trend observed for the RBAs, no clear pattern could be identified for the introduction of functional groups at C-16. Also, as observed for its binding affinity, the linkage of an anthracene group to ouabain's rhamnose moiety (anthrolyouabain) results in a minor increase in activity.

Table 2: Experimentally Determined Relative Binding Affinities and Relative Inhibitory Potencies of Cardiotonic Steroids<sup>a</sup>

compound name	RBA	RIP	RIP/RBA
ouabain	1.00 ± 0.37 <sup>b</sup>	1.00 ± 0.49	1.00
digoxin	2.13 ± 1.02	2.06 ± 1.16	1.04
digoxigenin	1.25 ± 0.84	1.25 ± 0.58	1.00
bisdigitoxoside			
digoxigenin	0.829 ± 0.148	1.07 ± 0.15	0.778
monodigitoxoside			
digoxigenin	11.1 ± 6.7	0.805 ± 0.399	13.8
bufalin	5.05 ± 2.35	0.142 ± 0.574	35.5
strophanthidin	10.4 ± 2.9	1.42 ± 0.10	7.31
ouabagenin	311 ± 152	2.21 ± 0.04	140
gitoxin	3.82 ± 0.83	1.17 ± 0.71	3.27
digitoxin	0.514 ± 0.256	0.611 ± 0.17	0.841
digitoxigenin	2.19 ± 0.70	0.515 ± 0.096	4.25
oleandrin	0.331 ± 0.091	0.858 ± 0.076	0.386
gitoxigenin	16.2 ± 6.2	0.746 ± 0.049	21.7
thetvetin B	7.25 ± 3.19	1.75 ± 0.05	4.14
chlormadinone acetate	147 ± 41	20.9 ± 7.2	7.05
cinobufagin	2.75 ± 0.56	0.144 ± 0.016	19.1
anthrolyouabain	0.449 ± 0.129	0.893 ± 0.757	0.503
helveticoside	39.5 ± 9.7	24.1 ± 0.6	1.63
digitoxigenin	0.448 ± 0.129	0.223 ± 0.026	2.01
bisdigitoxoside			
digitoxigenin	0.358 ± 0.116	0.174 ± 0.096	2.06
monodigitoxoside			
16-acetylgitoxin	3.35 ± 1.51	0.731 ± 0.109	4.58
gitoxigenin	2.78 ± 2.23	0.724 ± 0.729	3.84
3,16-diacetate			
α-methyldigoxin	3.31 ± 2.44	1.50 ± 0.977	2.21
α,β-diacetyldigoxin	2.25 ± 0.80	1.84 ± 1.32	1.22
strophanthidol	25.0 ± 10.2	1.40 ± 0.19	17.9
lanatoside A	0.723 ± 0.317	1.10 ± 0.09	0.655
evomonoside	0.127 ± 0.047	0.0607 ± 0.0273	2.03
dihydrodigoxin	146 ± 14	7.10 ± 1.00	20.6
uzarigenin	57.4 ± 24.4	1.36 ± 0.302	42.2
oleandrigenin	0.403 ± 0.059	0.555 ± 0.095	0.726
lanatoside C	2.57 ± 0.93	1.97 ± 0.19	1.31
peruvoside	0.247 ± 0.049	0.798 ± 0.054	0.309
proscillaridin A	0.446 ± 0.258	0.111 ± 0.016	4.01
neriifolin	0.138 ± 0.059	0.371 ± 0.009	0.372
cymarín	0.467 ± 0.103	0.927 ± 0.314	0.504
β-acetyldigoxin	1.31 ± 0.19	3.90 ± 0.423	0.336
dihydroouabain	22.9 ± 9.9	2.41 ± 1.44	9.52
lanatoside B	9.00 ± 3.68	0.843 ± 0.108	10.7

<sup>a</sup> Relative binding affinity (RBA) and relative inhibitory potency (RIP) are defined as the IC<sub>50</sub> value for a compound divided by the corresponding IC<sub>50</sub> value obtained for ouabain. Values are averages and standard deviations of three or more experimental trials. <sup>b</sup> The deviation for the RBA of ouabain is the standard deviation of all IC<sub>50</sub> values for this compound.

*Development of CoMSIA Models Describing Relative Binding Affinities and Inhibitory Potencies of Cardiac Glycosides.* For a detailed and rigorous analysis of the interactions that mediate binding specificity and inhibitory activities, we developed 3D-QSAR models using CoMSIA. The quality of the models for binding benefited significantly from the removal of helveticoside from the original data set of 37 observations. For unknown reasons, helveticoside displayed both a lower binding affinity and inhibitory potency than expected from its structure. In the case of ATPase inhibition, chlormadinone acetate was excluded from the model for similar reasons. As the only compound without a lactone component at C-17, chlormadinone acetate is structurally distinct from all the other tested inhibitors, and its

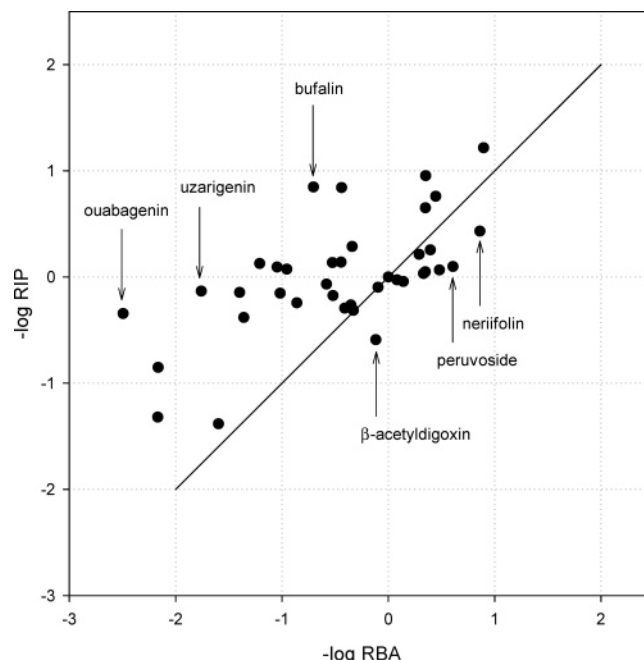


FIGURE 2: Correlation between experimentally determined binding affinities and inhibitory potencies of 37 cardiac glycosides. The three compounds with the highest RBA/RIP mismatches are identified and marked with arrows.

properties may therefore be poorly predicted by the 3D-QSAR models.

The PLS algorithm in SYBYL determined that three components were sufficient for the modeling of ligand binding, whereas the modeling of activity inhibition required five components. Further, the RBA values predicted by the binding model deviated from actual RBA values by a factor of no more than 10, while the predicted RIP values never differed from the actual ones by a factor of more than 3. Other parameters indicative of the quality of the models, such as the cross-validated correlation coefficient ( $r_{cv}$ ) and the conventional correlation coefficient ( $r_{ncv}$ ), were found to be within acceptable ranges [Supporting Information (Table 3)].

The CoMSIA model for cardiac glycoside binding indicated comparable relative contributions from the steric, electrostatic, and hydrophobic fields (12, 20, and 15%, respectively) and, interestingly, a large, dominant contribution from the two H-bond fields (combined, 52%). As a comparative method, though, CoMSIA addresses only *variations* in a given compound's property, such as the binding affinity, but does not quantify the nature of the overall driving force for binding. Therefore, the dominance of H-bonds only pertains to the fine-binding specificity of Na/K-ATPase, and it is not necessarily the principal driving force for cardiac glycosides' binding to the enzyme. The relative field contributions for the inhibition model were comparable to those for the binding model (8, 25, 17, and 49% for steric, electrostatic, hydrophobic, and combined H-bond fields, respectively).

Model validation was carried out by predicting the activities of external test compounds unknown to the models and showed that the developed models were capable of predicting the RBAs or RIPs of unknown compounds within 1 order of magnitude. It is also important that the statistical parameters obtained while excluding the test compounds were similar and thus independent of the selection of



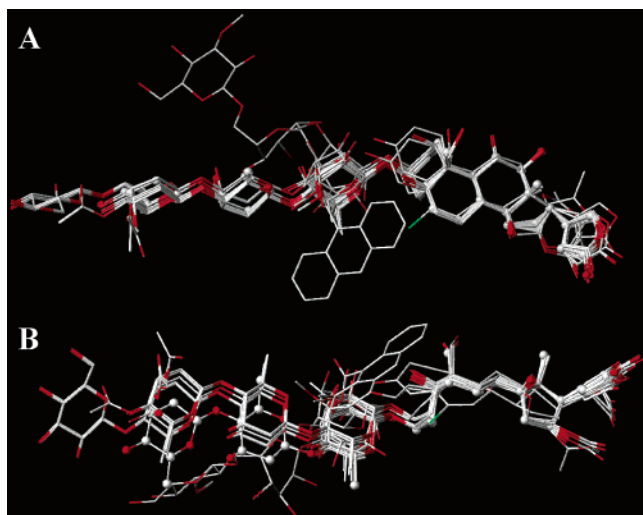


FIGURE 3: Alignment of the cardiac glycoside structures used for CoMSIA modeling. For visual clarity, only heavy atoms are shown. (A) “Top view” with respect to the steroid moiety. (B) Side view. As a reference, digoxin is shown as a ball-and-stick model.

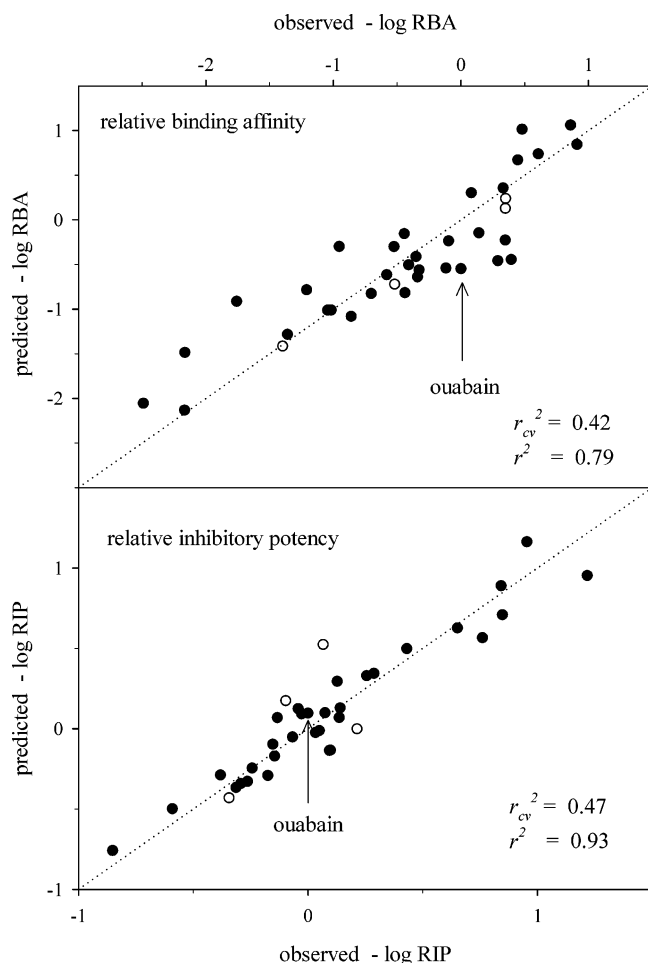


FIGURE 4: Correlation between CoMSIA-predicted and actual binding affinities (A) and inhibitory potencies (B) on a double-logarithmic scale. Empty circles indicate test set compounds that were excluded from the training set.

molecules assigned to the test set [Supporting Information (Table 3)]. The final models whose contour maps are shown in Figures 5–7 were derived by including all compounds (36 for binding and 35 for inhibition models).

## DISCUSSION

**3D-QSAR-Based Description of the Cardiac Glycoside Binding Site of Na/K-ATPase.** The scope of 3D-QSAR methodologies is the correlation of physical, chemical, or biological properties of compounds with their three-dimensional structures. Although initially developed for the *de novo* design of novel drugs, 3D-QSAR models have also provided accurate descriptions of ligand–receptor interactions where the three-dimensional structure of the receptor was unknown (22, 36, 41, 45). CoMFA and CoMSIA are widely used 3D-QSAR methods that express the structure of compounds in terms of molecular fields and link variations in compound activities with changes in the interaction energies in three-dimensional space (42). Compared to the older and more widely used steric and electrostatic CoMFA fields (43), CoMSIA facilitates a more comprehensive analysis of the types of ligand–receptor interactions involved by including hydrophobic and H-bond fields (25).

The steric contour map for cardiac glycoside binding to Na/K-ATPase (Figure 5A) reveals a green area about the  $\alpha$ -sugar, which indicates that the presence of steric bulk here increases ligand binding affinity. This is a reflection of the binding affinities peaking for the monosugar derivatives in the compound series that systematically vary the number of carbohydrates. Likely, the enzyme's binding site about this region is lined by amino acids that are capable of engaging in attractive van der Waals interactions with the inhibitors. On the other hand, the yellow contours about the  $\gamma$ -sugar indicate a sterically restricted area of interaction that is most likely partially occupied by amino acids of the enzyme as cardiac glycosides with three versus two sugar residues display a somewhat lowered binding affinity.

The contours in Figure 5C indicate electrostatic interactions that are dominated by a large blue area between the lactone ring and the steroid C-16 atom in which an increase in positive charge favors ligand binding. This contour is likely a consequence of the reduction in binding affinity observed upon introduction of hydroxyl groups at C-16 of the steroid. In addition, there is a small red area at the lactone ring in the proximity of the carbonyl group. Here, the presence of negative charge on the ligand improves binding and is likely the result of attractive electrostatic interactions between the carbonyl oxygen and positively charged counterparts of the Na/K-ATPase, such as protonated nitrogen atoms on Lys, Arg, Pro, and His side chains.

As suggested by the yellow hydrophobic contours (Figure 6A), the presence of polar groups in positions C-1 and C-19 at the steroid ring is detrimental to high-affinity binding. As a consequence, ouabagenin, strophanthidin, and strophanthidol display relatively low affinities. Interestingly, ouabain and cymarins, which also bear polar groups in these positions, still have high affinities. As discussed above, this is probably due to a compensation for the loss in affinity by their particular carbohydrate residue. Most likely, the region about C-1 and C-19 of the binding pocket is lined by residues such as Phe, Trp, Leu, Ile, or Val, giving this area a hydrophobic character. The gray contour about the  $\alpha$ -sugar, on the other hand, describes a region where polar groups on the ligand improve binding. This emphasizes the importance of the presence of at least one carbohydrate moiety for high binding affinity.



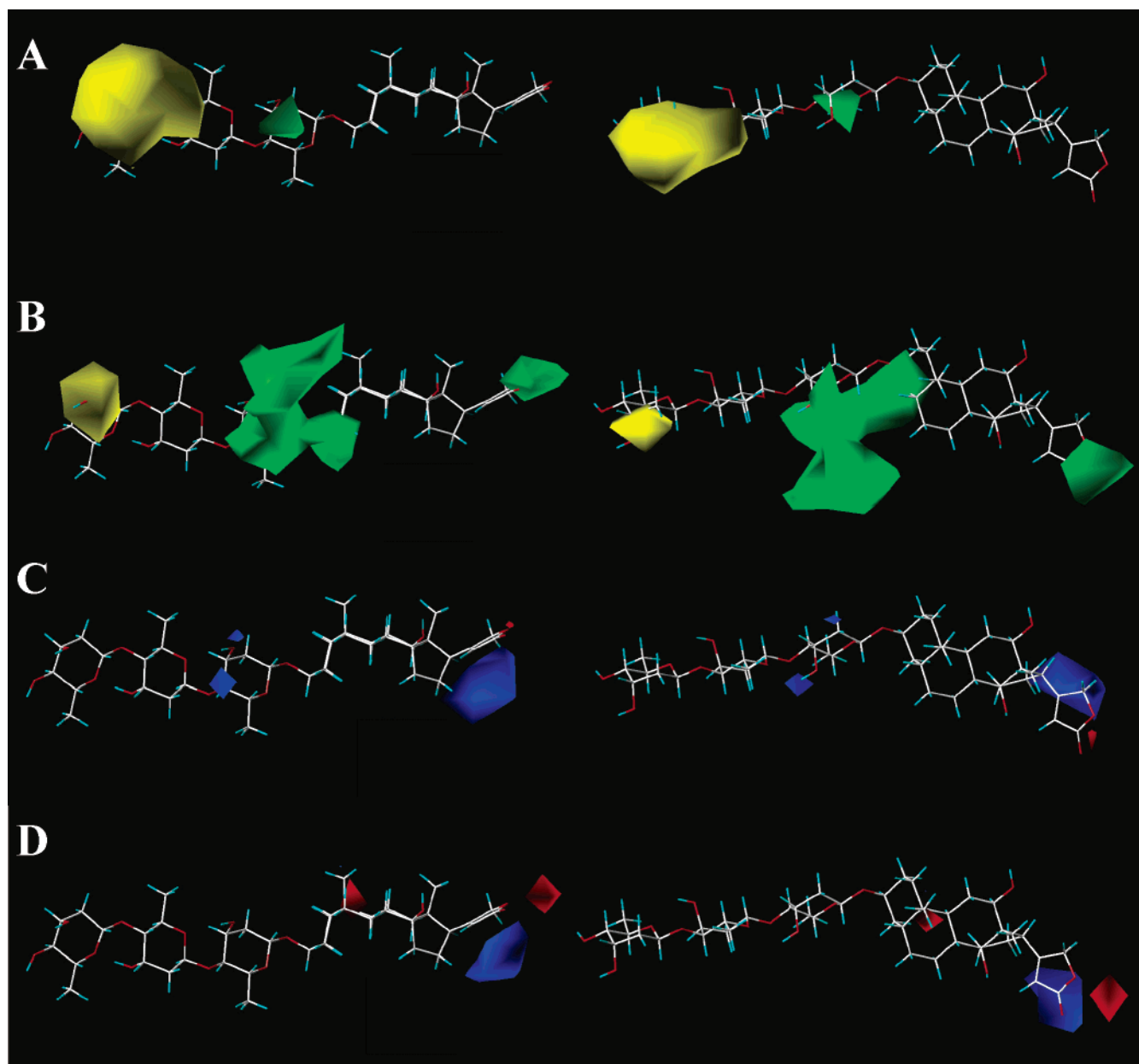


FIGURE 5: Orthographic views of the steric and electrostatic CoMSIA contour maps for ligand binding (A and C) and enzyme inhibition (B and D). The structure of digoxin is displayed as a reference. Activity increases upon addition of steric bulk on the cardiac glycoside in the green areas and decreases upon addition of steric bulk in the yellow areas (A and B). Activity increases upon addition of positive charge on the cardiac glycoside in the blue areas and decreases upon addition of positive charge in the red areas (C and D). Contour cutoff level of 88:12.

The H-bond donor contour map (Figure 7A) provides, for the first time, evidence for favorable interactions between H-bond-donating hydroxyl groups located in the proximity of substituents at C-4' on the  $\alpha$ -sugar and corresponding acceptor groups on the enzyme. This result reflects the high binding affinities displayed by compounds with one sugar moiety versus the corresponding genin and the slightly lower affinities of compounds whose sugar C-4' hydroxyl groups are part of a glycosidic bond and therefore prevented from engaging in H-bonds. Additional favorable interactions involving H-bonds are depicted in the H-bond acceptor map (Figure 7C), which suggests H-bonds between the ring oxygen of the  $\alpha$ -sugar and H-bond donor groups in the enzyme's binding site. The purple area in the proximity of C-1 and C-19 in Figure 7A is indicative of unfavorable interactions between the enzyme and the hydroxyl or

carbonyl groups of ouabagenin, strophanthidin, or strophanthidol in these positions. Likewise, the orange contours about the ring oxygen of the  $\gamma$ -sugar in Figure 7A are likely a result of the successive reduction in binding affinity upon addition of more carbohydrate moieties to the  $\alpha$ -sugar. Taken together, the shape of the H-bond contour maps and the relative dominance of the H-bond fields over the other CoMSIA fields stress the importance of the  $\alpha$ -carbohydrate moiety for high-affinity binding by Na/K-ATPase. These results appear to conflict with an earlier site-directed mutagenesis study (44, 45) that had ruled out interactions between the  $\alpha$ -carbohydrate moiety and side chains of amino acids on the H1–H2 loop. But, it should be noted that this report was based solely on the determination of ATPase activity inhibition, and the results may therefore not be relevant for high-affinity ligand binding.

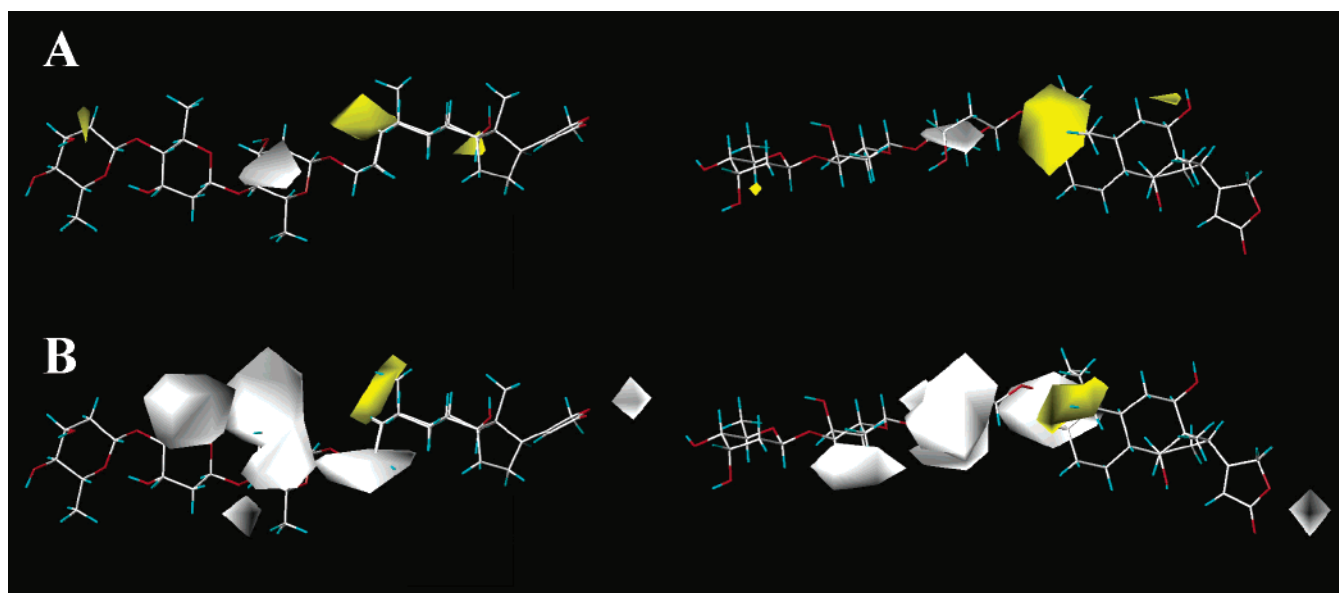


FIGURE 6: Orthographic view of the hydrophobic CoMSIA contour maps for ligand binding (A) and enzyme inhibition (B). The structure of digoxin is displayed as a reference. Activity increases with an increase in the hydrophobic character of the cardiac glycoside in the yellow areas and decreases with an increase in the hydrophobic character in the gray areas. Contour cutoff level of 88:12.

Finally, it should be noted that the CoMSIA maps display contours in all regions about the ligand that were probed by structural modifications (Figure 2). This implies that the digitalis binding site of Na/K-ATPase interacts with all major components of digoxin and must therefore be at least large enough to accommodate molecules the size of digoxin which, in an extended conformation, measures 27 Å in length. Therefore, the Na/K-ATPase digitalis binding pocket is considerably larger than that of other digitalis-specific “receptors”, such as mouse and human anti-digoxin monoclonal antibodies. The latter have been shown to interact primarily with the cardenolide moiety of cardiac glycosides, with the carbohydrates entirely or partially solvent-exposed and not involved in ligand binding (32, 33, 46).

**3D-QSAR-Based Comparison of Cardiac Glycoside Binding versus Inhibition of Na/K-ATPase Activity.** Despite considerable research efforts, the exact mechanisms of cardiac glycoside binding and inhibition of Na/K-ATPase remain elusive. Lingrel and co-workers (10, 13) proposed an inhibition model that postulates the involvement of the two hairpin loops connecting transmembrane helices 1 and 2 (H1–H2 loop) and 5 and 6 (H5–H6 loop). According to the model, these two loops are believed to have different functions. The H1–H2 loop is primarily responsible for the specific recognition of cardiac glycosides. Once bound to the enzyme, the cardiac glycoside then exerts its inhibitory activity by interacting at some point during the catalytic cycle with the H5–H6 loop and restricting its flexibility, a crucial property required for Na/K-ATPase function. If correct, this model implies that our measured binding affinities are primarily a reflection of interactions between cardiac glycosides and the H1–H2 loop, whereas the inhibitory potencies mainly describe the interactions of the glycosides and the H5–H6 loop. While ligand binding to the E<sub>2</sub>–P<sub>i</sub> form of Na/K-ATPase has the fastest on-rate and is believed to be accompanied by minor conformational changes, enzyme inhibition under turnover conditions is the result of interactions with the inhibitor at *any* point during the catalytic cycle, making the contributions of the resultant conformational

changes ambiguous. Therefore, binding affinity and inhibitory potency are not necessarily expected to follow the same trends. Furthermore, potassium ions are present in the activity assays because they are required for transport activity and they act as competitive inhibitors of cardiac glycosides, reducing the affinities of the latter and destabilizing the E<sub>2</sub>–P<sub>i</sub> conformation.

There is though considerable correlation between the two property values (RBA and RIP) and an overall resemblance of the contour maps for binding and inhibition (Figures 5–7). There are, however, some distinct differences. The most noticeable difference is visible in the steric parts of the contour maps (Figure 5A,B), which show, for activity inhibition, a favorable green area about the lactone ring. This feature is noticeably absent in the map for ouabain binding. This difference results from the enhanced inhibitory potency but lowered binding affinity upon enlargement of the five-membered lactone ring.

Whereas the exact locations and size of the contours vary to some extent, there is good agreement between the electrostatic (Figure 5C,D) and hydrophobic (Figure 6) contour maps for binding and inhibition. An exception is the presence of a gray contour region at the “right” side of the lactone ring (Figure 6B). This region is closest to polar atoms of the bufadienolides and provides an additional rationale for the enhanced inhibitory potency of this group of compounds.

In Figure 7, the H-bond donor map for activity inhibition shows an unfavorable area close to C-14, whereas the ligand binding map shows unfavorable areas in the proximity of C-1 and C-19. This is explained by the higher sensitivity of the binding affinity to introduction of hydroxyl groups about C-1 and C-19 (ouabagenin), whereas the inhibitory potency values are more sensitive to modifications at C-12. For the same reasons, the H-bond acceptor map for inhibition shows an unfavorable orange area about C-12 whereas the binding maps display none. Taken together, the areas in which CoMSIA locates exclusively inhibition interactions (lactone ring and C-12) may indicate the portion of the cardiac

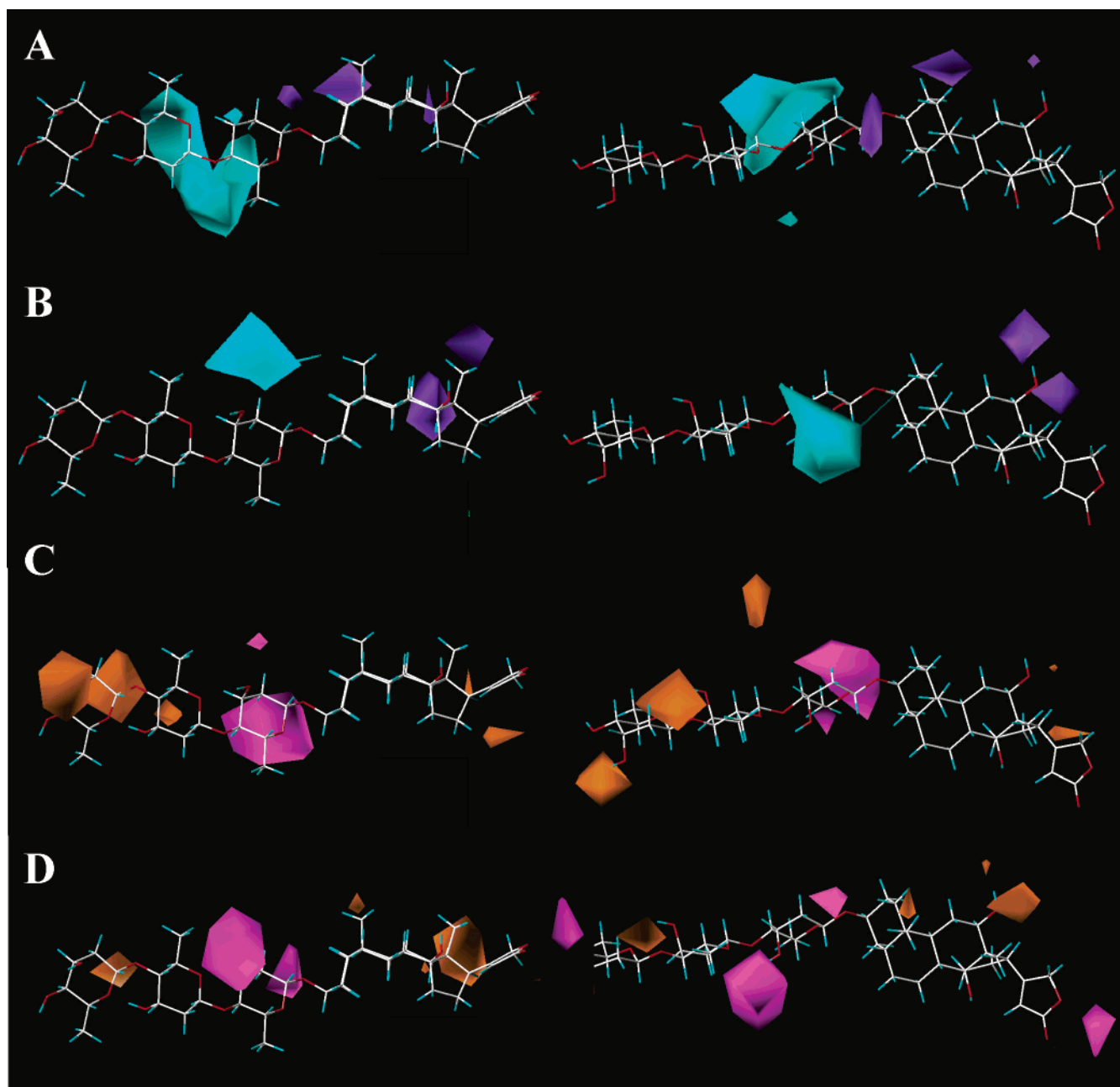


FIGURE 7: Orthographic view of the H-bond donor and the H-bond acceptor CoMSIA contour maps for ligand binding (A and C) and enzyme inhibition (B and D). The structure of digoxin is displayed as a reference. Activity increases with the presence of H-bond acceptor groups on the *receptor* in the cyan areas and decreases with the presence of H-bond acceptor groups in the purple areas (A and B). Activity increases with the presence of H-bond donor groups on the *receptor* in the cyan areas and decreases with the presence of H-bond donor groups in the orange areas (C and D). Contour cutoff level of 88:12.

glycosides that interact with the H5–H6 loop of the enzyme. Likewise, the region about C-1 and C-19 could be primarily involved in interactions with the H1–H2 loop.

Despite overlapping but nonidentical compound sets and the use of a different 3D-QSAR methodology, a comparison of the steric and electrostatic CoMSIA contour maps for activity inhibition shows good agreement with those of our previous CoMFA study (22). The favorable steric contours (green) are very similar, and the only difference relates to the unfavorable (yellow) region about the  $\gamma$ -sugar in the CoMSIA map. This is attributed to the fact that our earlier CoMFA study did not include as many structural variations in this area and was unable to recognize interactions at this location. The electrostatic maps are also in qualitative

agreement, although the CoMSIA map is less fragmented. This is an important and commonly observed feature that results from the use of Gaussian functions rather than of Lennard-Jones and Coulomb potentials which both have very steep distance dependencies (23, 24).

The compound that deserves special mention is ouabagenin because of the magnitude of its disparity between its binding and inhibition properties in comparison to those of ouabain. The large drop in ouabain's binding affinity upon removal of rhamnose is in sharp contrast to the small decrease in inhibitory potency. A possible explanation is that under  $Mg^{2+}/P_i$  binding conditions only inhibitor binding to the  $E_2$  conformation of Na/K-ATPase is monitored. In contrast, the turnover conditions of the ATPase activity assay allow for

interactions between the inhibitor and the receptor in all enzyme conformations ( $E_1$  and  $E_1'$ ) of the catalytic cycle. If, for some reason, the binding affinity of the enzyme for ouabagenin in the  $E_1$  but not  $E_2$  conformation were comparable to that of the other compounds, the high inhibitory potency would be the consequence because once bound, ouabagenin would still block the interconversion of intermediates. Clearly, more research is needed to understand ouabagenin's unique character.

**Design of a Digoxin Antagonist.** The cardiac glycosides digoxin and digitoxin have been in use for the treatment of CHF symptoms for more than 200 years and still are frequently prescribed drugs worldwide (1–6). A major disadvantage of digitalis is the narrow therapeutic index and the resultant risk for toxicity that can lead to life-threatening heart arrhythmias. Patients with such overdoses are injected with sheep polyclonal anti-digoxin antibody fragments (Digibind), which at present is the only available treatment for digitalis overdoses (47–49). However, the clinical use of these antibody fragments is limited because of concerns about adverse reactions to foreign species proteins.

An alternative remedy for the treatment of digitalis overdoses could be the administration of a competitive digoxin antagonist. Such a compound should block binding of digoxin to the Na/K-ATPase, but exert little or no effect on its function. Although this approach has not yet been applied to digitalis toxicity, the concept of such competitive antagonists has been established. For example, a number of studies have been aimed at finding a dopamine-sparing cocaine antagonist for the treatment of cocaine addiction (50–52). Another example is the use of drugs such as tamoxifen and raloxifene for the treatment of advanced breast cancer. These compounds act as competitive partial agonist inhibitors of estradiol at estrogen receptors (53).

For a digoxin antagonist to be effective, it needs to have a high affinity for the Na/K-ATPase binding site but a low inhibitory potency. Inspection of our CoMSIA contour maps shows that modifications of the lactone ring may be a good starting point for designing such a molecule. Replacement of the five-membered ring with a six-membered system causes opposite effects on binding and inhibition. Thus, a modification or reduction in ring size below the five-membered ring could result in a further improvement in binding affinity while reducing the inhibitory potency. Surprisingly, CoMSIA-based predictions for an ouabain analogue with a four-membered lactone ring yielded a lowered binding affinity and an essentially unchanged inhibitory potency. Apparently, it is not simply the size of the lactone ring that determines the biological activity but also the proper positioning of its functional groups, primarily of the two oxygen atoms, in their proper positions. Nevertheless, modifications at the lactone moiety still appear to be the most promising option because the binding–inhibition mismatches we observed in other regions of the cardiac glycoside skeleton are rather minor. Clearly, despite the inclusion of 37 compounds in our study, the exploration of possible structural changes and their effects on biological activities is certainly not complete and can be extended. For example, testing compounds with varying substituents about the steroid C-4, C-6, and C-7 positions or that contain only parts of the steroid ring system could identify additional

structural locations where differences in binding or inhibition may occur.

## ACKNOWLEDGMENT

We thank Purabi Dey for technical assistance and Dr. David Stanton for valuable discussions regarding the modeling of cardiac glycoside structures.

## SUPPORTING INFORMATION AVAILABLE

Statistical parameters of CoMSIA models. This material is available free of charge via the Internet at <http://pubs.acs.org>.

## REFERENCES

- Erdmann, E. (2000) The management of heart failure: An overview, *Basic Res. Cardiol.* 95, 13–17.
- Eichhorn, E. J., and Gheorghiade, M. (2002) Digoxin, *Prog. Cardiovasc. Dis.* 44, 251–266.
- Hauptman, P. J., and Kelly, R. A. (1999) Digitalis, *Circulation* 99, 1265–1270.
- Eichhorn, E. J., and Gheorghiade, M. (2002) Digoxin: New perspective on an old drug, *N. Engl. J. Med.* 347, 1394–1395.
- Li-Saw-Hee, F. L., and Lip, G. Y. H. (1998) Digoxin revisited, *Q. J. Med.* 91, 259–264.
- Nohria, A., Lewis, E., and Stevenson, L. W. (2002) Medical management of advanced heart failure, *JAMA, J. Am. Med. Assoc.* 287, 628–640.
- Møller, J. V., Juul, B., and le Maire, M. (1996) Structural organization, ion transport, and energy transduction of P-type ATPases, *Biochim. Biophys. Acta* 1286, 1–51.
- Jorgensen, P. L., and Pedersen, P. A. (2001) Structure–function relationships of  $\text{Na}^+$ ,  $\text{K}^+$ , ATP, or  $\text{Mg}^{2+}$  binding and energy transduction in Na,K-ATPase, *Biochim. Biophys. Acta* 1505, 57–74.
- Jorgensen, P. L., Hakansson, K. O., and Karlsh, S. J. (2003) Structure and mechanism of Na,K-ATPase: Functional sites and their interactions, *Annu. Rev. Physiol.* 65, 817–849.
- Lingrel, J. B., and Kuntzweiler, T. (1994)  $\text{Na}^+$ ,  $\text{K}^+$ -ATPase, *J. Biol. Chem.* 269, 19659–19662.
- Lingrel, J. B., Argüello, J. M., Van Huysse, J., and Kuntzweiler, T. A. (1997) Cation and cardiac glycoside binding sites of the Na,K-ATPase, *Ann. N.Y. Acad. Sci.* 834, 194–206.
- Wallick, E. T., Pitts, B. J. R., Lane, L. K., and Schwartz, A. (1980) A kinetic comparison of cardiac glycoside interactions with  $\text{Na}^+$ ,  $\text{K}^+$ /ATPases from skeletal and cardiac muscle and from kidney, *Arch. Biochem. Biophys.* 202, 442–449.
- Palasis, M., Kuntzweiler, T. A., Argüello, J. M., and Lingrel, J. B. (1996) Ouabain interactions with the H5–H6 hairpin of the Na,K-ATPase reveal a possible inhibition mechanism via the cation binding domain, *J. Biol. Chem.* 271, 14176–14182.
- Lee, A. G. (2002)  $\text{Ca}^{2+}$ -ATPase structure in the  $E_1$  and  $E_2$  conformations: Mechanism, helix–helix and helix–lipid interaction, *Biochim. Biophys. Acta* 1565, 246–266.
- Sagara, Y., Wade, J. B., and Inesi, G. (1992) A conformational mechanism for formation of a dead-end complex by the sarco-plasmic reticulum ATPase with thapsigargin, *J. Biol. Chem.* 267, 1286–1292.
- Repeke, K. R. H., Sweadner, K. J., Weiland, J., Megges, R., and Schön, R. (1996) In search of ideal inotropic steroids: Recent progress, *Prog. Drug Res.* 47, 9–52.
- Cerri, A., Serra, F., Ferrari, P., Folpini, E., Padoani, G., and Melloni, P. (1997) Synthesis, cardiotonic activity, and structure–activity relationships of  $17\beta$ -guanyldiazide derivatives of  $5\beta$ -androstane- $3\beta$ , $14\beta$ -diol acting on the  $\text{Na}^+$ ,  $\text{K}^+$ -ATPase receptor, *J. Med. Chem.* 40, 3484–3488.
- Cerri, A., Almirante, N., Barassi, P., Benicchio, A., Fedrizzi, G., Ferrari, P., Micheletti, R., Quadri, L., Ragg, E., Rossi, R., Santagostino, M., Schiavone, A., Serra, F., Zappavigna, M. P., and Melloni, P. (2000)  $17\beta$ O-Aminoalkyloximes of  $5\beta$ -androstane- $3\beta$ , $14\beta$ -diol with digitalis-like activity: Synthesis, cardiotonic activity, structure–activity relationships, and molecular modeling of the  $\text{Na}^+$ ,  $\text{K}^+$ -ATPase receptor, *J. Med. Chem.* 43, 2332–2349.
- Templeton, J. F., Ling, Y., Marat, K., and LaBella, F. S. (1997) Synthesis and structure–activity relationships of  $17\beta$ -substituted



- 14 $\beta$ -hydroxysteroid 3-( $\alpha$ -L-rhamnopyranoside)s: Steroids that bind to the digitalis receptor, *J. Med. Chem.* 40, 1439–1446.
20. Beer, J., Kunze, R., Herrmann, I., Portius, H. J., Mirsalichova, N. M., Abubakirov, N. K., and Repke, K. R. (1988) The thermodynamic essence of the reversible inactivation of Na<sup>+</sup>/K<sup>+</sup>-transporting ATPase by various digitalis derivatives is relaxation of enzyme conformational energy, *Biochim. Biophys. Acta* 937, 335–346.
  21. Schönfeld, W., Schönfeld, R., Menke, K. H., Weiland, J., and Repke, K. R. H. (1986) Origin of differences of inhibitory potency of cardiac glycosides in Na<sup>+</sup>/K<sup>+</sup>-transporting ATPase from human cardiac muscle, human brain cortex and guinea-pig cardiac muscle, *Biochem. Pharmacol.* 35, 3221–3231.
  22. Farr, C. D., Burd, C., Tabet, M. R., Wang, X., Welsh, W. J., and Ball, W. J., Jr. (2002) Three-dimensional quantitative structure–activity relationship study of the inhibition of Na/K-ATPase by cardiotonic glycosides, *Biochemistry* 41, 1137–1148.
  23. Klebe, G., Abraham, U., and Mietzner, T. (1994) Molecular similarity indices in a comparative analysis (CoMSIA) of drug molecules to correlate and predict their biological activity, *J. Med. Chem.* 37, 4130–4146.
  24. Klebe, G., and Abraham, U. (1999) Comparative molecular similarity index analysis (CoMSIA) to study hydrogen-bonding properties and to score combinatorial libraries, *J. Comput.-Aided Mol. Des.* 13, 1–10.
  25. Waller, C. L. (2004) Adding chemical information to CoMFA models with alternative 3D-QSAR fields, <http://www.netsci.org/Science/Compchem/feature10.html>.
  26. Lane, L. K., Potter, J. D., and Collins, J. H. (1997) Large-scale purification of Na,K-ATPase and its protein subunits from lamb kidney medulla, *Prep. Biochem.* 9, 157–170.
  27. Lowry, O. H., Rosebrough, N. J., Farr, A. L., and Randall, R. J. (1951) Protein measurement with the Folin phenol reagent, *J. Biol. Chem.* 193, 265–275.
  28. Schwartz, A., Allen, J. C., and Harigaya, S. (1969) Possible involvement of cardiac Na<sup>+</sup>/K<sup>+</sup>-adenosine triphosphatase in the mechanism of action of cardiac glycosides, *J. Pharmacol. Exp. Ther.* 168, 31–41.
  29. Wallick, E. T., and Schwartz, A. (1988) Interaction of cardiac glycosides with Na<sup>+</sup>/K<sup>+</sup>-ATPase, *Methods Enzymol.* 156, 201–213.
  30. Cheng, Y. C., and Prusoff, W. H. (1973) Relationship between the inhibition constant ( $K_i$ ) and the concentration of inhibitor which causes 50% inhibition ( $I_{50}$ ) of an enzymatic reaction, *Biochem. Pharmacol.* 22, 3099–3108.
  31. Schwartz, A., Allen, J. C., and Harigaya, S. (1969) Possible involvement of cardiac Na<sup>+</sup>/K<sup>+</sup>-adenosine triphosphatase in the mechanism of action of cardiac glycosides, *J. Pharmacol. Exp. Ther.* 168, 31–41.
  32. Jeffrey, P. D., Strong, R. K., Sieker, L. C., Chang, C. Y., Campbell, R. L., Petsko, G. A., Haber, E., Margolies, M. N., and Sherif, S. (1993) 26–10 Fab-digoxin complex: Affinity and specificity due to surface complementarity, *Proc. Natl. Acad. Sci. U.S.A.* 90, 10310–10314.
  33. Farr, C. D., Tabet, M. R., Ball, W. J., Jr., Fishwild, D. M., Wang, X., Nair, A. C., and Welsh, W. J. (2002) Three-dimensional quantitative structure–activity relationship analysis of ligand binding to human sequence antidigoxin monoclonal antibodies using comparative molecular field analysis, *J. Med. Chem.* 45, 3257–3270.
  34. Kawamura, A., Abrell, L. M., Maggiali, F., Berova, N., Nakanishi, K., Labutt, J., Magil, S., Haupt, G. T., and Hamlyn, J. M. (2001) Biological implications of conformational flexibility in ouabain, *Biochemistry* 40, 5835–5844.
  35. Bursi, R., Grootenhuys, A., van der Louw, J., Verhagen, J., de Gooyer, M., Jacobs, P., and Leysen, D. (2003) Structure–activity relationship study of human liver microsomes-catalyzed hydrolysis rate of ester prodrugs of MENT by comparative molecular field analysis (CoMFA), *Steroids* 68, 213–220.
  36. Paula, S., Tabet, M. R., Farr, C. D., Norman, A. B., and Ball, W. J., Jr. (2004) Three-dimensional quantitative structure–activity relationship modeling of cocaine binding by a novel human monoclonal antibody, *J. Med. Chem.* 47, 133–142.
  37. Viswanadhan, V. N., Ghose, A. K., Revankar, G. R., and Robins, R. K. (1989) Atomic physicochemical parameters for three-dimensional structure directed quantitative structure–activity relationships. 4. Additional parameters for hydrophobic and dispersive interactions and their application for an automated superposition of certain naturally occurring nucleoside antibiotics, *J. Chem. Inf. Comput. Sci.* 29, 163–172.
  38. Bush, B. L., and Nachbar, R. B. (1993) Sample-distance Partial Least Squares: PLS optimized for many variables, with application to CoMFA, *J. Comput.-Aided Mol. Des.* 7, 587–619.
  39. Wallick, E. T., Pitts, B. J., Lane, L. K., and Schwartz, A. (1989) A kinetic comparison of cardiac glycoside interactions with Na<sup>+</sup>/K<sup>+</sup>-ATPases from skeletal and cardiac muscle and from kidney, *Arch. Biochem. Biophys.* 202, 442–449.
  40. Schultheis, P. J., Wallick, E. T., and Lingrel, J. B. (1993) Kinetic analysis of ouabain binding to native and mutated forms of Na,K-ATPase and identification of a new region involved in cardiac glycoside interactions, *J. Biol. Chem.* 268, 22686–22694.
  41. Paula, S., Tabet, M. R., Keenan, S. M., Welsh, W. J., and Ball, W. J., Jr. (2003) Three-dimensional structure–activity relationship modeling of cocaine binding to two monoclonal antibodies by comparative molecular field analysis, *J. Mol. Biol.* 325, 515–530.
  42. Green, S. M., and Marshall, G. R. (1995) 3D-QSAR: A current perspective, *Trends Pharmacol. Sci.* 16, 285–291.
  43. Cramer, R. D., III, Patterson, D. E., and Bunce, J. D. (1988) Comparative molecular field analysis (CoMFA). I. Effect of shape on binding of steroids to carrier proteins, *J. Am. Chem. Soc.* 110, 5959–5967.
  44. O'Brien, W. J., Wallick, E. T., and Lingrel, J. B. (1993) Amino acid residues of the Na,K-ATPase involved in ouabain sensitivity do not bind the sugar moiety of cardiac glycosides, *J. Biol. Chem.* 268, 7707–7712.
  45. Carroll, I. F., Gao, Y., Rahman, M. A., Philip, A., Lewin, A. H., Boja, J. W., and Kuhar, M. J. (1991) Synthesis, ligand binding, QSAR and CoMFA study of 3 $\beta$ -(p-substituted phenyl)tropane-2 $\beta$ -carboxylic acid methyl esters, *J. Med. Chem.* 34, 2719–2725.
  46. Jeffrey, P. D., Schildbach, J. F., Chang, C. Y., Kussie, P. H., Margolies, M. N., and Sherif, S. (1995) Structure and specificity of the anti-digoxin antibody 40–50, *J. Mol. Biol.* 248, 344–360.
  47. Martiny, S. S., Phelps, S. J., and Massey, K. L. (1988) Treatment of severe digitalis intoxication with digoxin-specific antibody fragments: A clinical review, *Crit. Care Med.* 16, 629–635.
  48. Azrin, M. A. (1992) The use of antibodies in clinical cardiology, *Am. Heart J.* 124, 753–768.
  49. Hickey, A. R., Wenger, T. L., Carpenter, V. P., Tilson, H. H., Hlatky, M. A., Furberg, C. D., Kirkpatrick, C. H., Strauss, H. C., and Smith, T. W. (1991) Digoxin Immune Fab therapy in the management of digitalis intoxication: Safety and efficacy results of an observational surveillance study, *J. Am. Coll. Cardiol.* 17, 590–598.
  50. Carroll, F. I., Howell, L. L., and Kuhar, M. J. (1999) Pharmacotherapies for treatment of cocaine abuse: Preclinical aspects, *J. Med. Chem.* 42, 2721–2736.
  51. Slusher, B. S., Tiffany, C. W., Olkowski, J. L., and Jackson, P. F. (1997) Use of identical assay conditions for cocaine analog binding and dopamine uptake to identify potential cocaine antagonists, *Drug Alcohol Depend.* 48, 43–50.
  52. Cook, C. D., Carroll, F. I., and Beardsley, P. M. (1998) Separation of the locomotor stimulant and discriminative stimulus effects of cocaine by its C-2 phenyl ester analog, RTI-15, *Drug Alcohol Depend.* 50, 123–128.
  53. O'Regan, R. M., and Jordan, V. C. (2002) The evolution of tamoxifen therapy in breast cancer: Selective oestrogen-receptor modulators and downregulators, *Lancet Oncol.* 3, 207–214.

BI048680W